

## ELECTRONIC LETTER

## FRG1P is localised in the nucleolus, Cajal bodies, and speckles

S van Koningsbruggen, R W Dirks, A M Mommaas, J J Onderwater, G Deidda, G W Padberg, R R Frants, S M van der Maarel

*J Med Genet* 2004;41:e46 (<http://www.jmedgenet.com/cgi/content/full/41/4/e46>). doi: 10.1136/jmg.2003.012781

The highly conserved facioscapulohumeral muscular dystrophy (FSHD) region gene 1 (FRG1) was initially cloned as candidate gene of unknown function for FSHD. To explore the biological function of the FRG1 protein (FRG1P), we studied its cellular localisation in untransfected and FRG1 transfected cell lines. In interphase cells, FRG1P is localised in the dense structures of the nucleolus, in Cajal bodies, and in 60–80% of cells in nuclear speckles. A time course study revealed that FRG1P accumulates in nuclear speckles before its appearance in nucleoli, whereas the localisation in Cajal bodies remains unchanged, as does the localisation of NHPX protein. In accordance with the presence of FRG1P in these nuclear structures, transcription inhibition experiments showed an effect of RNA polymerases I and II on the localisation of FRG1P. Finally, by deletion of the predicted nuclear localisation signals of FRG1P, we demonstrated that both signals are necessary for this subnuclear localisation.

FRG1P is an attractive candidate for the pathogenesis of FSHD because of its high evolutionary conservation; its transcriptional deregulation in FSHD; and its colocalisation with proteins that are defective in the neuromuscular disorders oculopharyngeal muscular dystrophy (OPMD) and spinal muscular atrophy (SMA).

FRG1 (FSHD Region Gene 1, accession number L76159) was isolated as the first candidate gene for the autosomal dominant myopathy, facioscapulohumeral muscular dystrophy, in 1996.<sup>1</sup> FSHD is primarily characterised by progressive weakness and atrophy of the facial, upper arm, and shoulder muscles.<sup>2</sup> The FSHD locus on 4q35 contains a polymorphic repeat array consisting of 3.3 kb repeated elements (D4Z4). In control individuals, this array may vary between 11–100 units, whereas FSHD patients carry 1–10 units on one of their chromosomes 4, owing to the deletion of an integral number of D4Z4 units.<sup>3</sup> It is becoming increasingly evident that FSHD is caused by a local chromatin alteration, in which contraction of the D4Z4 repeat array results in the transcriptional deregulation of genes located on 4q35 (position effect). Indeed, Gabellini *et al* recently claimed evidence for transcriptional upregulation of genes close to the repeat in FSHD muscle, including FRG1.<sup>4</sup> In cultured cells, a transcriptional repressor complex binds to D4Z4, and partial loss of this complex leads to transcriptional upregulation of at least one 4qter gene, as observed in FSHD muscle. New expression data based on quantitative RT-PCR suggest that the expression of the 4q35 copy of FRG1 is in fact changed, although the nature of the deregulation is still controversial.<sup>5</sup>

FRG1P is highly conserved in vertebrates and non-vertebrates; the human protein is 97% identical to the murine protein and 46% identical to its orthologue in *C. elegans*.<sup>6</sup> Database searches have identified potential orthologues in—for example—*Drosophila*, tomato, *Xenopus* and *Schizosaccharomyces pombe*. As a result of multiple ectopic

## Key points

- Facioscapulohumeral muscular dystrophy (FSHD) is thought to be caused by a position effect mechanism in which contraction of the subtelomeric D4Z4 repeat on 4q35 results in the transcriptional deregulation of one or more 4qter genes.
- FRG1 is a suitable candidate gene because of its position close to the D4Z4 repeat, its high conservation, and its transcriptional deregulation in FSHD muscle.
- To obtain more insight into the function of FRG1 protein (FRG1P), its subcellular localisation was studied. FRG1P appears to be localised in the nucleolus, Cajal bodies, and speckles.
- These results are suggestive of a role for FRG1P in RNA processing. Interestingly, two other neuromuscular disorders, oculopharyngeal muscular dystrophy and spinal muscular atrophy, are also caused by defects in genes involved in RNA biogenesis.

duplications, in humans FRG1 belongs to a multigene family, with copies on many different chromosomes. The ancestral copy is located on chromosome 4q35, and is demonstrably transcribed in all tissues tested.<sup>1</sup> Additionally, this chromosome 4 copy of FRG1 is deregulated in FSHD muscle.<sup>4, 5</sup>

The FRG1 transcript is 1042 bp in length, and is distributed over nine exons encoding an open reading frame (ORF) of 258 amino acid residues.<sup>1</sup> This ORF is coding for a 30 kDa protein, which does not show homology to known proteins. Computer algorithms predict an amino terminal nuclear localisation signal (NLS) and a carboxy terminal bipartite (BP) nuclear localisation signal in FRG1P. In fact, the amino terminal signal consists of two NLS motifs, each four residues in size. Moreover, an imperfect lipocalin motif is predicted, which is involved in transport of hydrophobic particles.<sup>7</sup>

Despite its impressive conservation during evolution, indicating a fundamental function, little is known about the role of FRG1P. To obtain more insight into the biological function of FRG1P and its putative involvement in FSHD pathogenesis, we used immunological and GFP based techniques to study its subcellular localisation during different cell stages in untransfected and transfected cell lines. These studies demonstrate that FRG1P colocalises with PABPN1 and SMN1, both involved in related neuromuscular disorders.

## MATERIALS AND METHODS

## FRG1 fusion and deletion constructs

The ORF of FRG1 was amplified in 30 cycles from fibroblast cDNA using the primers 5'-CCGAGCTCATGGCCGAGTACTCC TATGTG-3' and 5'-CACTTGCAGTATCGATCGGCTTTTC-3',

and cloned in the TA cloning vector (Invitrogen, Carlsbad, CA, USA), which was subsequently used for all cloning strategies. Different tags were fused to FRG1P to control their effects on the localisation. A FLAG tag (pSupercatch-vector)<sup>8</sup> and a vesicular stomatitis tag (VSV, pSG8-vector)<sup>9</sup> were fused to the amino terminal end of FRG1P, to obtain pSG8VSV-FRG1 and pSC-FRG1, respectively. Additionally, the enhanced green fluorescent protein (EGFP, Clontech, Palo Alto, CA, USA) was fused both to the amino and the carboxy terminal ends of FRG1P (pEGFP-FRG1).

All deletion constructs were derived from pSG8VSV-FRG1. The  $\Delta 1$  construct, FRG1 without NLS, was obtained by deletion of amino acid 4–81. Subsequently, the  $\Delta 2$  construct, FRG1 without BP, and the  $\Delta 3$  variant, FRG1 without NLS and BP signals, were generated by deletion of amino acid 232–257 or 4–81, and 232–257, respectively. Finally, the  $\Delta 4$  deletion construct, missing amino acid 47–231, contained only the NLS and the BP sequences.

All constructs were sequence verified using the BigDye terminator sequencing kit (Perkin Elmer; Foster City, CA, USA) and analysed on an ABI377 (Perkin Elmer). Extensive cloning strategies are available on request.

### Cell culture

COS-1 cells, human rhabdomyosarcoma cell line TE671 (gift from Dr A Belayew, Mons, Belgium), and the osteosarcoma cell line U2OS were maintained in DMEM without phenol red (GIBCO Invitrogen, Breda, Netherlands, or GIBCO-BRL), supplemented with 10% fetal bovine serum (FBS) (GIBCO-BRL), L-glutamine (2 mM, GIBCO-BRL), glucose (100x, GIBCO-BRL), and penicillin–streptomycin (100 IU/100 µg/ml, GIBCO-BRL). The murine myogenic cell line C2C12 was cultured in the same medium, supplemented with 20% FBS. The cells were cultured in an incubator with 5% CO<sub>2</sub> at 37°C.

### Transient and stable transfections

Twenty four hours before transient transfections,  $1 \times 10^5$  COS-1, TE671, and U2OS cells, and  $2.5 \times 10^4$  C2C12 cells were seeded per 35 mm culture dish, with or without coverslips ( $20 \times 20$  mm). Cells were transfected using Fugene (Roche, Basel, Switzerland), according to the manufacturer's instructions.

For stable transfections,  $7 \times 10^5$  U2OS cells were seeded in 9 cm dishes and transfected with pEGFP-FRG1, according to the Fugene protocol. Twenty four hours after transfection, cells were put under selection by adding 400 µg/ml Geneticin (G418, GIBCO-BRL). After two to three weeks, genetic resistant colonies were selected and screened for the expression of EGFP-FRG1P. Clones 3 and D were used for further experiments.

For the time course experiment, COS-1 cells were transiently transfected with pEGFP-FRG1 and fixed at every two hours from one to 19 hours, and at 24, 48, 72, and 120 hours. After staining with appropriate Cajal body and speckle markers, 50 cells at each time point were analysed for the localisation of EGFP-FRG1P.

### Total cell lysates and nuclear extracts

U2OS cells were lysed with Laemmli buffer to obtain total cell lysates. Nuclear and cytoplasmic extracts were obtained from  $2 \times 10^7$  untransfected and EGFP-FRG1P stably transfected U2OS cells (clones 3 and D), as previously described.<sup>10</sup> Protein concentrations were measured using the Pierce kit (Pierce, Rockford, IL, USA), according to the manufacturer's instructions.

### Antibodies

Two polyclonal rabbit anti-FRG1P sera were raised against recombinant FRG1P (124987 and 124988). Both were able to

detect overexpressed FRG1P in immunological assays. Anti-serum 124987 performed better than 124988 and was therefore used in all subsequent experiments. Anti-FRG1P serum was used in 1:1000 dilution on Western blot and for immunocytochemistry, and the affinity purified rabbit anti-FRG1P antibody (derived from anti-serum 124987) was used in 1:10 dilution for all applications.

For immunocytochemistry and immunoblotting, the mouse monoclonal M2 anti-FLAG antibody (Sigma-Aldrich, St Louis, MO, USA) and P5D4 (gift from Dr J Franssen, Nijmegen, Netherlands) were used in a dilution of 1:5000 and 1:3000, respectively. Colocalisation studies were performed with mouse anti-fibrillarin (1:5) (gift from Dr KM Pollard, Scripps Institute, San Diego, USA), mouse anti-SC35 (1:500) (Sigma-Aldrich), mouse anti-coilin (1:200) (gift from Dr A I Lamond, Dundee, UK), and mouse anti-PML 5E10 (1:10) (gift from Dr L de Jong, Amsterdam, Netherlands). The purity of the nuclear and cytoplasmic fractions were confirmed with mouse anti-beta tubulin E7 (DSHB, Iowa, USA) in a dilution of 1:5, and with rabbit anti-PABPN1 (gift from Dr E Wahle, Halle, Germany), in a dilution of 1:200. Rabbit anti-mouse Alexa<sup>594</sup> (Molecular Probes, Eugene, OR, USA) and goat anti-mouse<sup>cy5</sup> were used in 1:1000 and 1:500 dilutions for immunocytochemistry. For immunoblotting, goat anti-mouse<sup>HRP</sup> and goat anti-rabbit<sup>HRP</sup> (Jackson Laboratory, West Grove, PA, USA) were used in dilutions of 1:1000 and 1:5000, respectively. Immuno electron microscopy (immunoEM) was performed with P5D4 and rabbit anti-mouse in dilutions of 1:6000 and 1:200, respectively. The antibody complex was detected with protein-A 10 nm gold in a dilution of 1:400.

### Protein induction in BL21-CodonPlus (De3) bacteria

pET28-FRG1(-NLS) induction was performed according to the manufacturer's instructions (Stratagene, La Jolla, CA, USA). Bacterial cells were dissolved in sonic buffer (300 mM sodium chloride, 50 mM sodium phosphate, pH 8.0) after three hours and lysed using a French press (American Instrument Company, Haverhill, MA, USA). The lysate was centrifuged for 30 minutes at 7000 g, to obtain the soluble FRG1P-NLS fraction in the supernatant.

### Antibody affinity purification

The polyclonal rabbit anti-FRG1P serum was incubated with one volume of soaked ammonium sulphate for 30 minutes on ice, and centrifuged for 12 minutes at 7000 g to remove serum albumin. The pellet was resuspended in a 1:3 starting volume of sonic buffer at pH 8.0, with a 1:3 starting volume of soaked ammonium sulphate, and incubated again for 30 minutes on ice. This procedure was repeated twice. Finally, the pellet was resuspended in a 2:3 starting volume sonic buffer at pH 8.0.

HIS-FRG1P(-NLS) bacterial lysates were bound to talon resin (Clontech) according to the manufacturer's instructions, before the serum and the talon were incubated overnight at 4°C. Anti-FRG1P antibodies were eluted by 6 M guanidine in sonic buffer at pH 8.0. Finally, purified proteins were dialysed against PBS three times for at least one hour each time.

### Immunoblotting

Lysates were loaded on a 10% SDS-polyacrylamide gel and blotted onto Hybond-ECL membrane (Amersham, Amersham, UK). Immunoblotting was performed according to standard protocols. The blot was incubated with the primary P5D4 antibody and the secondary goat anti-mouse<sup>HRP</sup>, for 60 minutes each. Protein bands were visualised using the Amersham ECL kit, according to the manufacturer's instructions.

## Immunocytochemistry

Cells were fixed and permeabilised in 4% formaldehyde (Merck, Darmstadt, Germany)/0.1% triton X-100 for 20 minutes at RT. Before incubation with the primary antibody for one hour, formaldehyde groups were blocked with 0.1 M ammonium chloride for 10 minutes. Cells were washed twice in PBS/1% BSA (Sigma-Aldrich) between every step. After incubation with the secondary antibody for one hour, cells were washed twice in PBS, dehydrated in a graded ethanol series, and mounted in DAPI (50 ng/ $\mu$ l) vectashield (Vector Laboratories, Burlingame, CA, USA). Final preparations were analysed with a Leica Aristoplan fluorescence microscope, and images were obtained using Cytovision (Applied Imaging, Santa Clara, CA, USA) digital system.

## Electron microscopy

COS-1 cells were trypsinised, washed in PBS, fixed in 0.1% glutaraldehyde in 0.14 M cacodylate buffer (pH 7.3) for one hour, and processed for immunogEM as described elsewhere.<sup>11</sup> Immunolabelling was performed with P5D4, rabbit-anti-mouse and protein A-10 nm gold.

## Transcription inhibition

Transcription in stably transfected FRG1 cell lines was inhibited by actinomycin D (Sigma-Aldrich) at concentrations of 0.04, 0.2, 1, 5, and 20  $\mu$ g/ml three hours before fixation, or by incubating the cells for 90 minutes or three hours with 5,6-dichlorobenimidazole ribose (DRB) (Sigma-Aldrich) at a concentration of 25  $\mu$ g/ml.

## RESULTS

### The endogenous FRG1P is located in the nucleus

Total, nuclear, and cytoplasmic extracts of untransfected and two EGFP-FRG1P stably transfected U2OS cell lines (3 and D) were analysed on Western blot to demonstrate that the endogenous FRG1P is localised in nuclei, in accordance with the predicted NLS and BP signals. As expected, beta tubulin and PABPN1 were predominantly detected in the cytoplasmic and nuclear fractions, respectively (fig 1). The endogenous FRG1P was clearly detected in the nuclear fractions, but not in the cytoplasmic fractions of each cell line. At a very low level, the postimmune anti-FRG1P serum also detected FRG1P in total cell lysates (fig 1). As expected, the preimmune serum did not show reactivity for FRG1P (fig 1). In addition, EGFP-FRG1P was clearly detected with both the postimmune anti-FRG1P serum and the anti-GFP antibody, and was mainly restricted to the nuclear extracts of both stably transfected cell lines (fig 1).

Since the antiserum failed to visualise the endogenous FRG1P in immunofluorescent assays of cell lines and tissue, we could not study endogenous FRG1P in muscle of patients and controls. Therefore, transient and stable transfections were performed to study its subcellular localisation in more detail.

### The subcellular localisation of FRG1P fusion constructs

Initially, all full length expression constructs of the FRG1P fusion proteins were transiently transfected in different cell types: COS-1, U2OS, and the myogenic cell lines C2C12 and TE671. Since all these transient transfections showed a similar distribution of the FRG1 fusion protein, EGFP-FRG1 was subsequently stably transfected in U2OS cells. All cell lysates were analysed on Western blot to confirm expression of the full length FRG1P fusion proteins. Both the anti-tag antibodies and the affinity purified polyclonal anti-FRG1P antibody clearly detected the fusion proteins of the correct sizes (fig 1). In stably transfected cells, immunofluorescent assays showed FRG1P to be localised in nucleoli and in small nuclear bodies during interphase. A diffuse nuclear localisation was also apparent (fig 2). In mitotic cells, which were

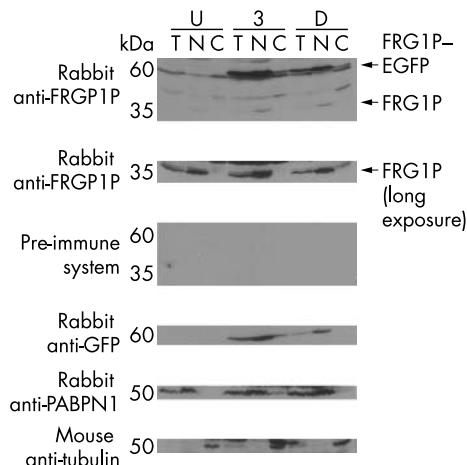


**Figure 1** Western blot analysis of total (T), nuclear (N), and cytoplasmic (C) extracts of untransfected (U) and EGFP-FRG1P stably transfected (3 and D) U2OS cell lines. The rabbit anti-FRG1P antiserum, but not the preimmune serum, detected FRG1P in nuclear extracts and at very low levels in total cell lysates upon longer exposure. The lower panels show the same extracts stained with rabbit anti-GFP, rabbit anti-PABPN1 (nuclear), and mouse anti-tubulin (cytoplasmic).

devoid of nuclei, FRG1P was localised throughout the whole cell. Identical localisation signals were obtained after transient transfections, using different expression constructs in various cell lines. Remarkably, in approximately 60–80% of the transiently transfected cells, FRG1P was also localised in a nuclear speckle-like structure. The subnuclear localisation was consistent in all cells studied, even in cells expressing the transgene at very low, presumably close to endogenous, levels.

### FRG1P, a predominantly nucleolar protein, is associated with dense nucleolar structures

The nucleolar localisation was evident from negative DAPI staining, and confirmed by double immunostaining with the known nucleolar protein fibrillarin (fig 2A–D).<sup>12</sup> Furthermore, immunogEM showed a clear labelling of the nucleolus in COS-1 cells transfected with pSG8VSV-FRG1 (fig 3A). FRG1P localisation was restricted to the dense structures of the nucleolus (dense fibrillar component and granular component) (fig 3B).

### FRG1P is also detected in Cajal bodies and in nuclear speckles

Double staining of FRG1P and coilin, a Cajal body marker, identified the small FRG1P-positive nuclear structures as Cajal bodies (fig 2E–H).<sup>13</sup> Such a colocalisation was not seen for promyelocytic leukaemia (PML) bodies using antibodies specific for PML protein (data not shown).<sup>14</sup> The additional speckle-like structures in which FRG1P was found following transient transfections were defined as splicing factors containing domains, or nuclear speckles, by double staining with the splicing factor SC35 (fig 2I–L).<sup>15</sup>

### Localisation of nuclear speckles precedes nucleolar staining

To study the trafficking of FRG1P between these nuclear components, COS-1 cells were transiently transfected with pEGFP-FRG1 and fixed at intervals of two hours from one to 19 hours, and at 24, 48, 72, and 120 hours after transfection. Seven hours after transfection, EGFP-FRG1P was detected in the nuclear speckles and in Cajal bodies, which was again confirmed by double staining with antibodies against SC35 and coilin, respectively. After nine hours, FRG1P was also

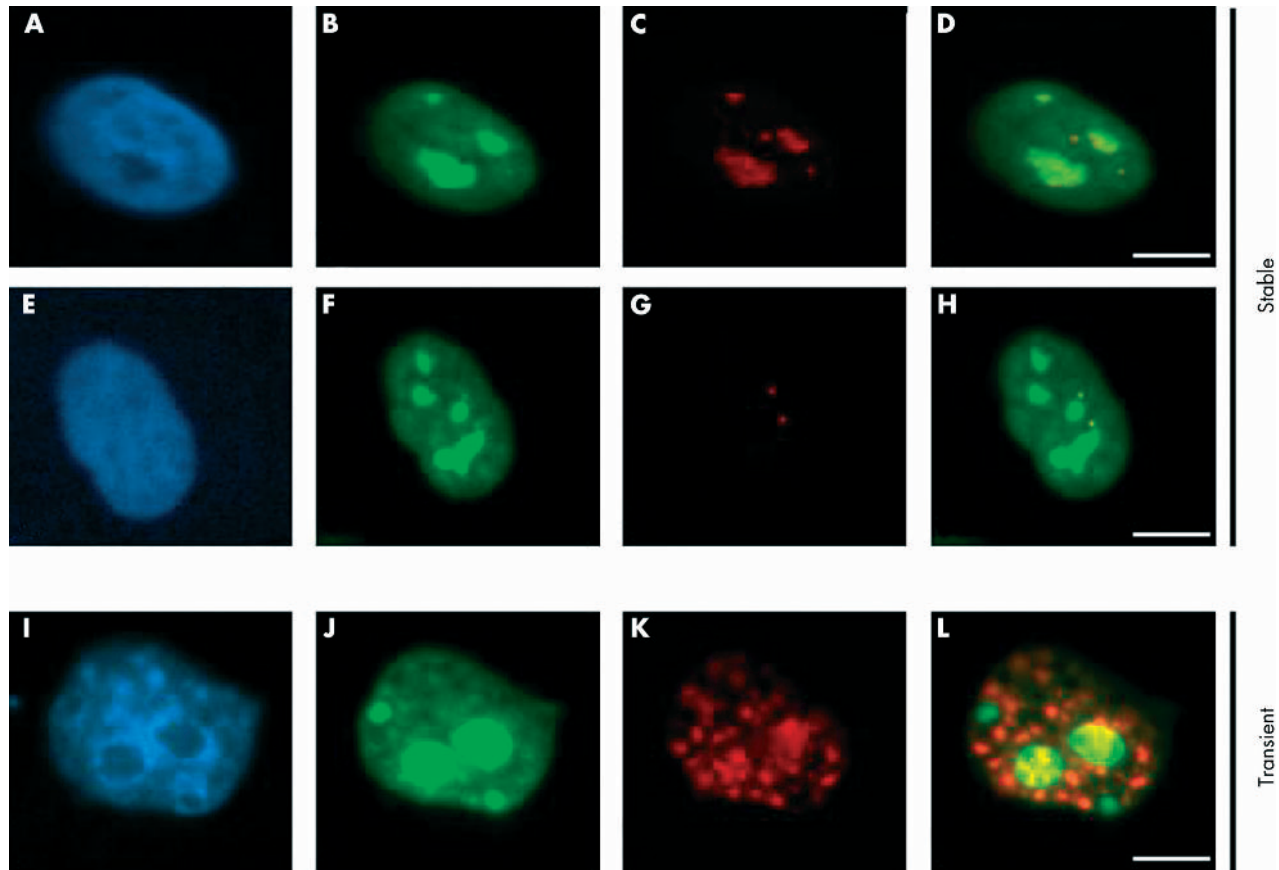


**Figure 2** Stable transfections of EGFP-FRG1 in U2OS cells (A–H), and a transient transfection of EGFP-FRG1 in COS-1 cells (I–L). (A), (E), and (I), DAPI staining demonstrating the nucleus with a negative staining of the nucleoli. (B, F), Stable U2OS cells expressing EGFP-FRG1P. (C) Nucleolar and Cajal body localisation of fibrillarlin. (D) Merging B and C shows colocalisation in nucleoli and Cajal bodies. (G) Cajal body localisation of coilin. (H) Merging both images F and G shows colocalisation in Cajal bodies. (J) EGFP-FRG1P expression in transiently transfected COS-1 cells. (K) Speckle localisation of SC35. (L) Merging (J) and (K) shows colocalisation in the nuclear speckles. Bar = 10  $\mu$ m.

slightly expressed in the nucleoli of some cells. Over time, the amount of cells expressing FRG1P in nucleoli increased, whereas the speckle staining decreased. However, the speckle

localisation did not completely disappear in all cells. In contrast, the Cajal body staining remained stable over time. The dynamic localisation of FRG1P is shown in fig 4.

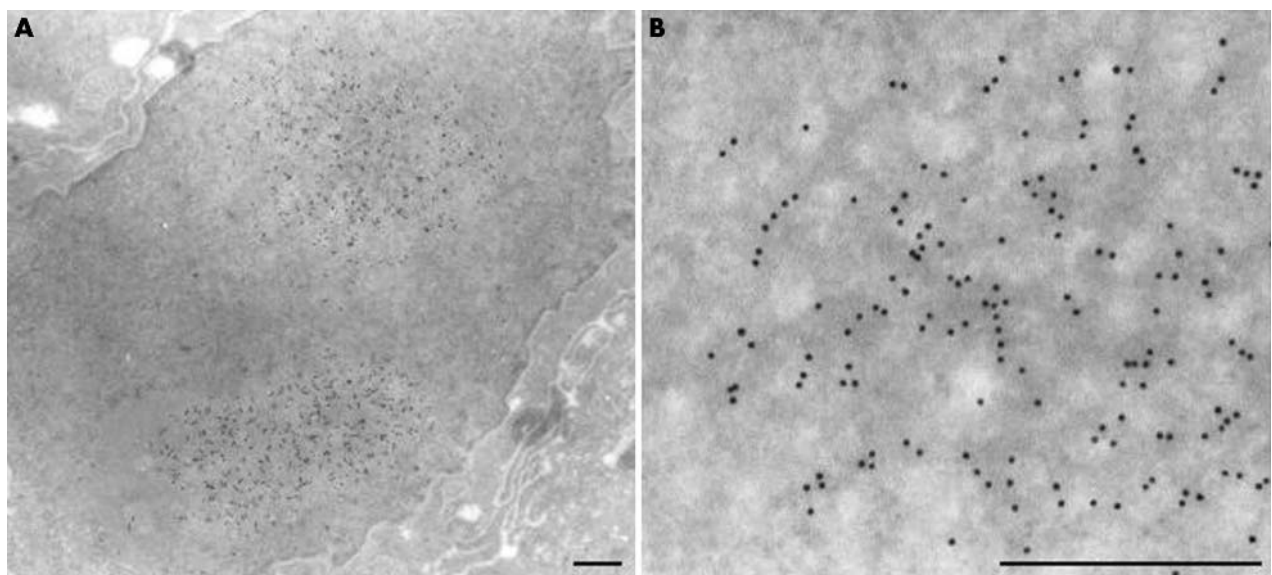


**Figure 3** Electron micrographs of ultrathin cryosections of transiently transfected COS-1 cells. VSV-FRG1P was visualised by P5D4 antibody and 10 nm colloidal gold. (A) FRG1P labelling is restricted to the nucleoli. (B) A higher magnification shows that FRG1P is localised to the dense areas of the nucleoli (DFC and GC). Bar = 0.5  $\mu$ m.

### FRG1 has two nuclear localisation signals

To test the functionality of the putative nuclear signals in FRG1P, deletion constructs of pSG8VSV-FRG1 were generated (fig 5A). These constructs were either missing the amino terminal NLS ( $\Delta 1$ ) or the carboxy terminal BP ( $\Delta 2$ ) or both signals ( $\Delta 3$ ). In a fourth construct ( $\Delta 4$ ), the region between both signals was removed. The protein sizes of the different deletion constructs were analysed by Western blot and proved to be correct (fig 5B). Transient transfection of these deletion constructs in COS-1 cells showed that  $\Delta 1$ , without NLS, displayed a diffuse nuclear and cytoplasmic staining (fig 5C). The  $\Delta 2$  construct, lacking the BP, revealed a nuclear speckle localisation (fig 5D), which was confirmed by colocalisation with SC35 (data not shown). Deletion of the NLS and BP signals ( $\Delta 3$ ) resulted in a diffuse nuclear and cytoplasmic localisation (fig 5E). Finally, the construct containing only the NLS and the BP ( $\Delta 4$ ) was localised in nucleoli and speckles, like the full length FRG1 construct (fig 5F).

### Transcription inhibition suggests a role for FRG1P in RNA biogenesis

To study the role of FRG1P in RNA processing, transcription inhibition experiments were performed in U2OS cells stably transfected with EGFP-FRG1. Addition of low concentrations of actinomycin D (0.02 and 0.04  $\mu\text{g/ml}$ ) resulted in accumulation of EGFP-FRG1P at the nucleolar periphery, but the localisation of FRG1P in the Cajal bodies remained unchanged (fig 6A–B). Treatment with high concentrations of actinomycin D (5 and 20  $\mu\text{g/ml}$ ) or DRB caused redistribution of FRG1P from the nucleoli and Cajal bodies to the nucleoplasm (fig 6C–F).

### DISCUSSION

FRG1 was isolated as a positional candidate gene for the autosomal dominant myopathy FSHD, but the function of the encoded protein product is still unknown and a role in FSHD pathogenesis is not yet established.<sup>1</sup> Nevertheless, the presence of highly conserved FRG1 homologues in vertebrates and non-vertebrates is suggestive of an essential role in evolution.<sup>6</sup>

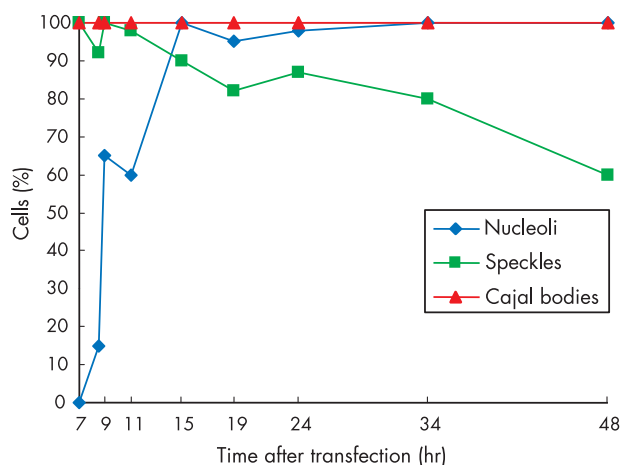


**Figure 4** Representation of the dynamic localisation of FRG1P after transient transfection in COS-1 cells. Cells are fixed at different time intervals after transfection (X axis), and the number of cells expressing FRG1P in Cajal bodies, nucleoli, or speckles is shown as the percentage of the total number of transfected cells analysed (Y axis). At each time interval, 50 cells were inspected for the localisation of FRG1P.

As a first step towards understanding the function of the encoded protein FRG1P, we studied its subcellular localisation in more detail. FRG1P probably is not an abundant protein, since it can only be detected at very low levels on Western blots of total lysates. Since immunofluorescent assays failed to detect FRG1P in different cell lines and muscle sections of patients and controls, we studied its subcellular localisation in cell lines transfected with FRG1 using immunocytochemistry and immunocytochemistry. All our studies demonstrated that FRG1P is localised in nucleoli and Cajal bodies, as evidenced by colocalisation experiments with fibrillarin and coilin. In 60–80% of the transiently transfected cells, FRG1P was also localised in the nuclear speckles, demonstrated by a double staining with SC35.

The membraneless nucleolus is involved in rRNA processing, ribosome assembly,<sup>16–17</sup> maturation of small nuclear ribonucleolar proteins (snRNPs),<sup>18–19</sup> and nuclear export of a subset of mRNAs.<sup>18–20</sup> Our immunocytochemistry studies provided evidence that FRG1P is localised in the dense structures of the nucleolus—that is, the dense fibrillar component and the granular component—which may be indicative of a role in processing of pre-rRNA or in assembly of rRNA into ribosomal subunits.<sup>16–17–21</sup> Indeed, low concentrations actinomycin D, affecting RNA polymerase I (pol I), cause accumulation of EGFP-FRG1P at the nucleolar periphery, as described for coilin, fibrillarin, and GARI.<sup>22–23</sup>

FRG1P is also localised in Cajal bodies, which are nuclear structures of 0.2–1.5  $\mu\text{m}$  in size and varying in number from 1–10 per cell. Cajal bodies contain a variety of components, including splicing snRNPs and small nucleolar RNPs (snoRNPs), and human autoantigen P80-coilin.<sup>24–25</sup> They are thought to be involved in post-transcriptional modification of spliceosomal snRNAs and snoRNAs,<sup>19–26–28</sup> and in shuttling snRNPs from the nucleoplasm to the nucleolus.<sup>29–30</sup> As expected, transcription inhibition of RNA polymerase II (pol II) with high concentrations of actinomycin D or DRB redistributes FRG1P from nucleoli and Cajal bodies to the nucleoplasm.

Lastly, transiently transfected cells revealed the presence of FRG1P in nuclear speckles, which may serve as storage sites for protein splicing factors and snRNPs. They may also coordinate transcription and RNA processing.<sup>31</sup> The presence of FRG1P in nuclear speckles after transient transfection could be the result of elevated FRG1P expression. Conversely, the absence of FRG1P in the speckle domains in stably transfected cells is a reflection of low expression.

Interestingly, a novel nucleolar pathway was recently described, in which newly synthesised NHPX protein was localised in the nuclear speckles before accumulation in nucleoli, whereas the Cajal body localisation remained unchanged.<sup>32</sup> The human NHPX protein is a homologue of NHP2p and orthologue of Snu13p, both from *Saccharomyces cerevisiae*.<sup>33–35</sup> NHPX was demonstrated to be involved both in late stage spliceosome assembly and in rRNA cleavage/modification by binding to U4 snRNA and box C/D snoRNAs, respectively.<sup>36–38</sup> Our time course experiment also demonstrated that the nucleolar localisation of FRG1P was preceded by a transient speckle accumulation, whereas this protein was expressed in Cajal bodies at all time points. Therefore, the speckle localisation of FRG1P might well be caused by an overload of the same pathway as described for NHPX. After acute overexpression, FRG1P can probably not be transported fast enough from the speckles and therefore accumulates. In the light of these results, we hypothesise that, like NHPX, newly synthesised endogenous FRG1P is localised in speckles and Cajal bodies, whereas the mature protein is present in nucleoli and Cajal bodies.

In accordance with its localisation, two nuclear localisation signals were predicted in FRG1P, an aminoterminal NLS

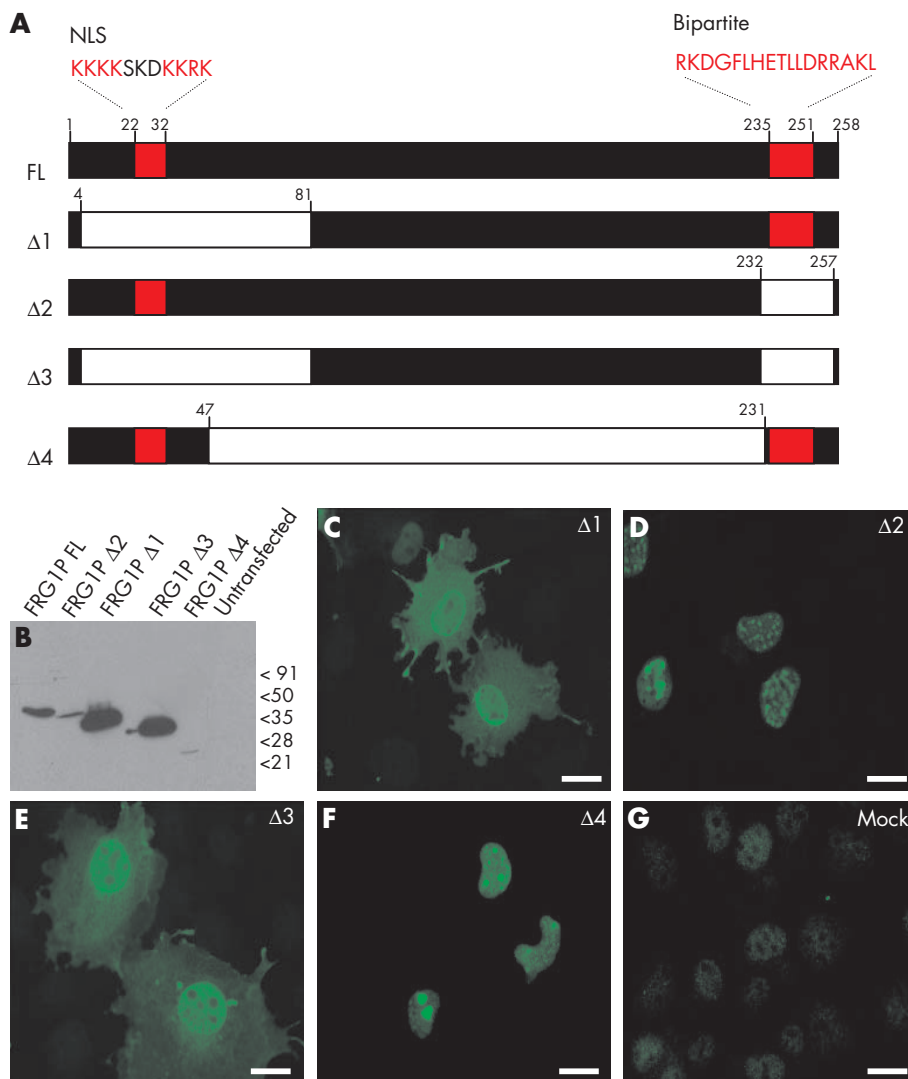


**Figure 5** Deletion construct of pSG8VSV-FRG1. (A) Schematic representation of full length FRG1P and the different FRG1 deletion constructs (Δ1–Δ4). The NLS and bipartite signals are marked in red and the amino acid positions are indicated above the constructs. (B) Western blot of total lysates from COS-1 cells, which were transiently transfected with full length FRG1P and the different FRG1 deletion constructs. (C–G) Immunocytochemical analysis of transiently transfected COS-1 cells with deletion constructs of pSG8VSV-FRG1. (C) Δ1, the construct missing the NLS, shows a diffuse nuclear and cytoplasmic staining. (D) Δ2, without the BP signal, is localised in speckles. (E) Δ3, missing both the NLS and BP, displays nuclear and cytoplasmic staining. (F) Δ4, the construct missing the region between the NLS and the BP, shows the same pattern as the full length FRG1P. (G) Mock transfection with the empty pSG8VSV vector does not show any signal. Bar = 20 μm.

(KKKK at position 22–25 and KKRK) and a carboxyterminal BP signal (amino acids 235–251).<sup>39–40</sup> No specific nucleolar localisation (NoLS) signals have been described, but probably a long array of basic amino acids flanked by basic amino acids, RXXR motifs (in which the X is preferably an arginine or leucine), or RGG motifs, may act as NoLS.<sup>41–44</sup> The basic amino acid arrays in FRG1P may thus act as NLS and NoLS. By deletion of either or both of the nuclear localisation signals, we showed that the NLS alone was sufficient for a nuclear localisation of FRG1P, but both NLS and BP were necessary for nucleolar localisation.

The subcellular localisation of FRG1P and its redistribution upon transcription inhibition suggest a possible role in rRNA or mRNA processing.<sup>25–45</sup> This is substantiated by the detection of FRG1P in a large scale human spliceosome analysis<sup>46</sup> and by the coordinate expression of FRG1P with other proteins involved in ribosomal and mRNA biogenesis in *C. elegans*.<sup>47</sup>

Remarkably, two other neuromuscular disorders are caused by defects in proteins involved in RNA biogenesis. First, the late onset dominant myopathy OPMD typically presents, like FSHD, with a non-limb-girdle phenotype. OPMD is caused by a moderate alanine expansion in the N-terminus of PABPN1, leading to aggregation of PABPN1 in intranuclear filamentous inclusions in a subset of muscle nuclei.<sup>48–49</sup> In the nucleus, PABPN1 is localised in speckles and nucleoli, where it stimulates and controls the synthesis of poly(A) tails of pre-mRNA. Although these aggregates in OPMD show many parallels with those caused by polyglutamine expansions,<sup>50</sup> impaired mRNA biogenesis in OPMD cannot be excluded, since the N-terminus of PABPN1 is essential for the stimulation of poly(A) polymerase and it has been demonstrated that these aggregates sequester poly(A) RNA.<sup>49–51</sup>

Secondly, SMA is caused, in many cases, by disruption of the telomeric copy of the duplicated SMN genes.<sup>52</sup> The SMN

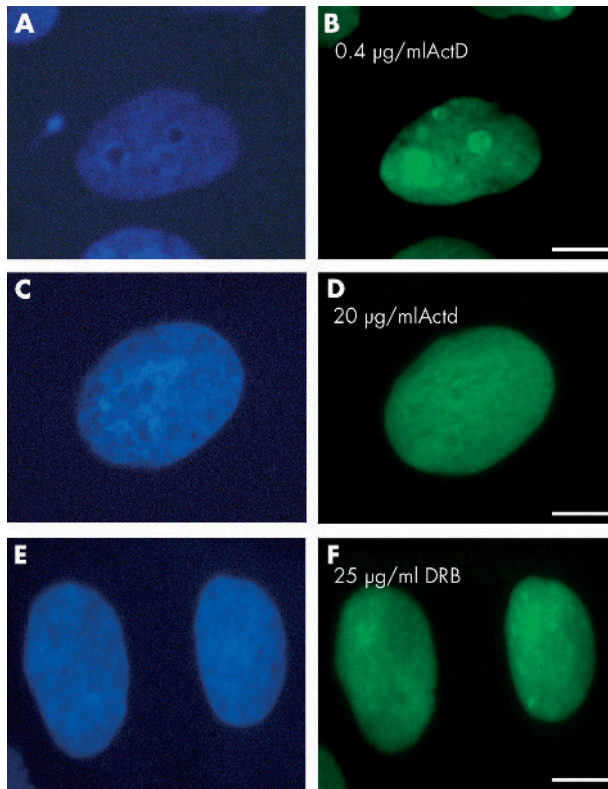


**Figure 6** Transcription inhibition with actinomycin D (ActD) (A–D), and with DRB (E–F), in stably transfected EGFP-FRG1P U2OS cells. (A), (C), and (E) DAPI staining demonstrating the nucleus with a negative staining of the nucleoli. (B) EGFP-FRG1P is localised at the nucleolar periphery and in Cajal bodies after treatment with 0.04 µg/ml ActD for three hours. (D) A diffuse nuclear staining after treatment with 20 µg/ml ActD for three hours. (F) EGFP-FRG1P is localised in the nucleoplasm after treatment with 25 µg/ml DRB for three hours. Bar = 10 µm.

protein is involved in spliceosome biogenesis and pre mRNA splicing, and is localised in the cytosol and in gems, nuclear domains closely associated with or completely overlapping with Cajal bodies. Despite the knowledge about its function, the mechanism leading to SMA remains unclear. SMA is characterised by degeneration of the motor neurones in the spinal cord leading to muscle atrophy. In addition, several studies indicate that the SMA phenotype also results from constitutive skeletal muscle defects.<sup>53–56</sup>

Nevertheless, more experiments will be required to identify protein and/or RNA partners of FRG1P to elucidate its putative role in RNA biogenesis and FSHD pathology. As FSHD is not caused by mutations in a specific gene, but rather acts through ectopic expression of one or more genes in the vicinity of D4Z4, identification of the FSHD gene will depend on functional analysis of deregulated 4qter genes. It has been postulated that highly conserved genes that require a strict transcriptional stoichiometry are most susceptible to these position effects.<sup>57</sup> Therefore, the close proximity of the FRG1 gene to D4Z4, its transcriptional deregulation, its evolutionary conservation, and the subcellular colocalisation of the encoded protein with other proteins involved in related disorders, warrant further investigation of its role in FSHD.

#### ACKNOWLEDGEMENTS

We thank Dr C T Verrips, representing the FSHD Foundation, for providing the means to generate the polyclonal anti-FRG1P antibody; Dr A M J M van den Maagdenberg for his constructive comments; and Dr A K Raap for critically reading the manuscript.

Our research was funded by the Princess Beatrix Fund, the Muscular Dystrophy Association (USA), the Dutch FSHD Foundation, the National Institutes of Health of the European Union, and the FSH Society, USA.

#### Authors' affiliations

**S van Koningsbruggen, R R Frants, S M van der Maarel**, Department of Human Genetics, Leiden University Medical Center, Netherlands  
**R W Dirks**, Department of Molecular Cell Biology, Leiden University Medical Center, Netherlands  
**A M Mommaas, J J Onderwater**, Centre for Electron Microscopy, Leiden University Medical Center, Netherlands  
**G Deidda**, Institute of Cell Biology, CNR, Rome, Italy  
**G W Padberg**, Department of Neurology, University Medical Center Nijmegen, Netherlands

Correspondence to: S M van der Maarel, Leiden University Medical Center, MGC-Department of Human Genetics, Wassenaarseweg 72, 2333 AL Leiden, Netherlands; maarel@lumc.nl

#### REFERENCES

- 1 **van Deutekom JCT**, Lemmers RILF, Grewal PK, van Geel M, Romberg S, Dauwerse HG, Wright TJ, Padberg GW, Hofker MH, Hewitt JE, Frants RR. Identification of the first gene (*FRG1*) from the FSHD region on human chromosome 4q35. *Hum Mol Genet* 1996;**5**:581–90.
- 2 **Padberg GW**. Facioscapulohumeral disease. Thesis. Netherlands: Leiden University, 1982.
- 3 **Wijmenga C**, Hewitt JE, Sandkuijl LA, Clark LN, Wright TJ, Dauwerse HG, Gruter AM, Hofker MH, Moerer P, Williamson R, van Ommen GJ, Padberg GW, Frants RR. Chromosome 4q DNA rearrangements associated with facioscapulohumeral muscular dystrophy. *Nat Genet* 1992;**2**:26–30.
- 4 **Gabellini D**, Green M, Tupler R. Inappropriate gene activation in FSHD. A repressor complex binds a chromosomal repeat deleted in dystrophic muscle. *Cell* 2002;**110**:248–339.
- 5 **Jiang G**, van Overveld PG, Yang F, Vedanarayanan V, van der Maarel SM, Ehrlich M. Testing the position-effect variegation hypothesis for facioscapulohumeral muscular dystrophy by analysis of histone modification and gene expression in subtelomeric 4q. *Hum Mol Genet* 2003;**12**(22):2909–21.
- 6 **Grewal PK**, Carim Todd L, van der Maarel S, Frants RR, Hewitt JE. FRG1, a gene in the FSH muscular dystrophy region on human chromosome 4q35, is highly conserved in vertebrates and invertebrates. *Gene* 1998;**216**:13–19.
- 7 **Flower DR**. The lipocalin protein family: structure and function. *Biochem J* 1996;**318**:1–14.
- 8 **Georgiev O**, Bourquin JP, Gstaiger M, Knoepfel L, Schaffner W, Hovens C. Two versatile eukaryotic vectors permitting epitope tagging, radiolabelling and nuclear localisation of expressed proteins. *Gene* 1996;**168**:165–7.
- 9 **Cuppen E**, Gerrits H, Pepers B, Wieringa B, Hendriks W. PDZ motifs in PTP-BL and RIL bind to internal protein segments in the LIM domain protein RIL. *Mol Biol Cell* 1998;**9**:671–83.
- 10 **Waisfisz Q**, de Winter JP, Kruyt FA, de Groot J, van der Weel L, Dijkmans LM, Zhi Y, Arwert F, Scheper RJ, Youssoufian H, Hoatlin ME, Joenje H. A physical complex of the Fanconi anemia proteins FANCG/XRCC9 and FANCA. *Proc Natl Acad Sci U S A* 1999;**96**:10320–5.
- 11 **Mommaas AM**, Wijsman MC, Mulder AA, van Praag MC, Vermeer BJ, Koning F. HLA class II expression on human epidermal Langerhans cells in situ: upregulation during the elicitation of allergic contact dermatitis. *Hum Immunol* 1992;**34**:99–106.
- 12 **Aris JP**, Blobel G. cDNA cloning and sequencing of human fibrillarlin, a conserved nucleolar protein recognized by autoimmune antisera. *Proc Natl Acad Sci U S A* 1991;**88**:931–5.
- 13 **Ogg SC**, Lamond AI. Cajal bodies and coilin—moving towards function. *J Cell Biol* 2002;**159**:17–21.
- 14 **Eskiw CH**, Bazett-Jones DP. The promyelocytic leukemia nuclear body: sites of activity? *Biochem Cell Biol* 2002;**80**:301–10.
- 15 **Spector DL**, Fu XD, Maniatis T. Associations between distinct pre-mRNA splicing components and the cell nucleus. *EMBO J* 1991;**10**:3467–81.
- 16 **Melese T**, Xue Z. The nucleolus: an organelle formed by the act of building a ribosome. *Curr Opin Cell Biol* 1995;**7**:319–24.
- 17 **Scheer U**, Hock R. Structure and function of the nucleolus. *Curr Opin Cell Biol* 1999;**11**:385–90.
- 18 **Pederson T**. The plurifunctional nucleolus. *Nucleic Acids Res* 1998;**26**:3871–6.
- 19 **Sleeman J**, Lyon CE, Platani M, Kreivi JP, Lamond AI. Dynamic interactions between splicing snRNPs, coiled bodies and nucleoli revealed using snRNP protein fusions to the green fluorescent protein. *Journal of Cell Science Supplement* 1998;**243**:290–304.
- 20 **Bond VC**, Wold B. Nucleolar localisation of myc transcripts. *Genome Res* 1993;**13**:3221–30.
- 21 **Hannan KM**, Hannan RD, Rothblum LI. Transcription by RNA polymerase I. *Front Biosci* 1998;**3**:376–98.
- 22 **Raska I**, Ochs RL, Andrade LE, Chan EK, Burlingame R, Peebles C, Gruol D, Tan EM. Association between the nucleolus and the coiled body. *J Struct Biol* 1990;**104**:120–7.

- 23 **Pellizzoni I**, Baccon J, Charroux B, Dreyfuss G. The survival of motor neurones (SMN) protein interacts with the snoRNP proteins fibrillarin and GAR1. *Curr Biol* 2001;**11**:1079–88.
- 24 **Sleeman JE**, Lamond AI. Nuclear organization of pre-mRNA splicing factors. *Curr Opin Cell Biol* 1999;**11**:372–7.
- 25 **Carmo-Fonseca M**. New clues to the function of the Cajal body. *EMBO Rep* 2002;**3**:726–7.
- 26 **Narayanan A**, Speckmann W, Terns R, Terns MP. Role of the box C/D motif in localisation of small nucleolar RNAs to coiled bodies and nucleoli. *Mol Biol Cell* 1999;**10**:2131–47.
- 27 **Darzacq X**, Jady BE, Verheggen C, Kiss AM, Bertrand E, Kiss T. Cajal body-specific small nuclear RNAs: a novel class of 2'-O-methylation and pseudouridylation guide RNAs. *EMBO J* 2002;**21**:2746–56.
- 28 **Verheggen C**, Lafontaine DL, Samarsky D, Mouaikel J, Blanchard JM, Bordonne R, Bertrand E. Mammalian and yeast U3 snoRNPs are matured in specific and related nuclear compartments. *EMBO J* 2002;**21**:2736–45.
- 29 **Bohmann K**, Ferreira JA, Lamond AI. Mutational analysis of p80 coilin indicates a functional interaction between coiled bodies and the nucleolus. *J Cell Biol* 1995;**131**:817–31.
- 30 **Bohmann K**, Ferreira J, Santama N, Weis K, Lamond AI. Molecular analysis of the coiled body. *J Cell Sci Suppl* 1995;**19**:107–13.
- 31 **Dirks RW**, Hattinger CM, Molenaar C, Snaar SP. Synthesis, processing, and transport of RNA within the three-dimensional context of the cell nucleus. *Crit Rev Eukaryot Gene Expr* 1999;**9**:191–201.
- 32 **Leung AK**, Lamond AI. In vivo analysis of NHPX reveals a novel nucleolar localisation pathway involving a transient accumulation in splicing speckles. *J Cell Biol* 2002;**157**:615–29.
- 33 **Saito H**, Fujiwara T, Shin S, Okui K, Nakamura Y. Cloning and mapping of a human novel cDNA (NHP2L1) that encodes a protein highly homologous to yeast nuclear protein NHP2. *Cytogenet Genome Res* 1996;**72**:191–3.
- 34 **Kolodrubetz D**, Burgum A. Sequence and genetic analysis of NHP2: a moderately abundant high mobility group-like nuclear protein with an essential function in *Saccharomyces cerevisiae*. *Yeast* 1991;**7**:79–90.
- 35 **Gottschalk A**, Neubauer G, Banroques J, Mann M, Luhrmann R, Fabrizio P. Identification by mass spectrometry and functional analysis of novel proteins of the yeast [U4/U6.U5] tri-snoRNP. *EMBO J* 1999;**18**:4535–48.
- 36 **Nottrott S**, Hartmuth K, Fabrizio P, Urlaub H, Vidovic I, Ficner R, Luhrmann R. Functional interaction of a novel 15.5 kD [U4/U6.U5] tri-snoRNP protein with the 5' stem-loop of U4 snRNA. *EMBO J* 1999;**18**:6119–33.
- 37 **Vidovic I**, Nottrott S, Hartmuth K, Luhrmann R, Ficner R. Crystal structure of the spliceosomal 15.5 kD protein bound to a U4 snRNA fragment. *Mol Cell* 2000;**6**:1331–42.
- 38 **Watkins NJ**, Segault V, Charpentier B, Nottrott S, Fabrizio P, Bachi A, Wilm M, Rosbash M, Branlant C, Luhrmann R. A common core RNP structure shared between the small nucleolar box C/D RNPs and the spliceosomal U4 snRNP. *Cell* 2000;**103**:457–66.
- 39 **Dingwall C**, Laskey RA. Nuclear targeting sequences—a consensus? *Trends Biochem Sci* 1991;**16**:478–81.
- 40 **Robbins J**, Dilworth SM, Laskey RA, Dingwall C. Two interdependent basic domains in nucleoplasmic nuclear targeting sequence: identification of a class of bipartite nuclear targeting sequence. *Cell* 1991;**64**:615–23.
- 41 **Dang CV**, Lee WM. Nuclear and nucleolar targeting sequences of c-erb-A, c-myc, N-myc, p53, HSP70, and HIV tat proteins. *J Biol Chem* 1989;**264**:18019–23.
- 42 **Liu JL**, Lee LF, Ye Y, Qian Z, Kung HJ. Nucleolar and nuclear localisation properties of a herpesvirus bZIP oncoprotein, MEQ. *J Virol* 1997;**71**:3188–96.
- 43 **Das A**, Park JH, Hagen CB, Parsons M. Distinct domains of a nucleolar protein mediate protein kinase binding, interaction with nucleic acids and nucleolar localisation. *J Cell Sci* 1998;**111**:2615–23.
- 44 **Quaye IK**, Toku S, Tanaka T. Sequence requirement for nucleolar localisation of rat ribosomal protein L31. *Eur J Cell Biol* 1996;**69**:151–5.
- 45 **Tollervey D**, Lehtonen H, Jansen R, Kern H, Hurt EC. Temperature-sensitive mutations demonstrate roles for yeast fibrillarin in pre-rRNA processing, pre-rRNA methylation, and ribosome assembly. *Cell* 1993;**72**:443–57.
- 46 **Rappsilber J**, Ryder U, Lamond AI, Mann M. Large-scale proteomic analysis of the human spliceosome. *Genome Res* 2002;**12**:1231–45.
- 47 **Kim SK**, Lund J, Kiraly M, Duke K, Jiang M, Stuart JM, Eizinger A, Wylie BN, Davidson GS. A gene expression map for *Caenorhabditis elegans*. *Science* 2001;**293**:2087–92.
- 48 **Brais B**, Bouchard JP, Xie YG, Rochefort DL, Chretien N, Tome FM, Lafreniere RG, Rommens JM, Uyama E, Nohira O, Blumen S, Korczyn AD, Heutink P, Mathieu J, Duranceau A, Codere F, Fardeau M, Rouleau GA, Korczyn AD. Short GCG expansions in the PABP2 gene cause oculopharyngeal muscular dystrophy. (Published erratum appears in *Nat Genet* 1998; **19**(4):404.) *Nat Genet* 1998;**18**:164–7.
- 49 **Calado A**, Tome FM, Brais B, Rouleau GA, Kuhn U, Wahle E, Carmo-Fonseca M. Nuclear inclusions in oculopharyngeal muscular dystrophy consist of poly(A) binding protein 2 aggregates which sequester poly(A) RNA. *Hum Mol Genet* 2000;**9**:2321–8.
- 50 **Bao YP**, Cook LJ, O'Donovan D, Uyama E, Rubinsztein DC. Mammalian, yeast, bacterial, and chemical chaperones reduce aggregate formation and death in a cell model of oculopharyngeal muscular dystrophy. *J Biol Chem* 2002;**277**:12263–9.
- 51 **Kuhn U**, Nemeth A, Meyer S, Wahle E. The RNA binding domains of the nuclear poly(A)-binding protein. *J Biol Chem* 2003;**278**:16916–25.
- 52 **Nicole S**, Cifuentes-Diaz C, Frugier T, Melki J. Spinal muscular atrophy: recent advances and future prospects. *Muscle Nerve* 2002;**26**:4–13.
- 53 **Nicole S**, Desforges B, Millet G, Lesbordes J, Cifuentes-Diaz C, Vertes D, Cao ML, De Backer F, Languille L, Roblot N, Joshi V, Gillis JM, Melki J. Intact satellite cells lead to remarkable protection against Smn gene defect in differentiated skeletal muscle. *J Cell Biol* 2003;**161**(3):571–82.
- 54 **Henderson CE**, Hauser M, Huchet F, Dessi F, Hentati F, Tagushi T, Changeux JP, Fardeau M. Extracts of muscle biopsies from patients with spinal muscular atrophies inhibit neurite outgrowth from spinal neurones. *Neurology* 1987;**37**:1361–4.
- 55 **Braun S**, Croizat B, Lagrange MC, Warter JM, Pointron P. Constitutive muscular abnormalities in culture in spinal muscular atrophy. *Lancet* 1995;**345**:694–5.
- 56 **Cifuentes-Diaz C**, Frugier T, Tiziano FD, Lacene E, Roblot N, Joshi V, Moreau MH, Melki J. Deletion of murine SMN exon 7 directed to skeletal muscle leads to severe muscular dystrophy. *J Cell Biol* 2001;**152**:1107–14.
- 57 **Engelkamp D**, van Heyningen V. Transcription factors in disease. *Curr Opin Genet Dev* 1996;**6**:334–42.